

Electron-beam-irradiation effects in bulk $\text{YBa}_2\text{Cu}_3\text{O}_{7-x}$

S. N. Basu,^{a)} T. E. Mitchell, and M. Nastasi
Los Alamos National Laboratory, Los Alamos, New Mexico 87545

(Received 10 September 1990; accepted for publication 22 November 1990)

Irradiation effects on thin foils of bulk $\text{YBa}_2\text{Cu}_3\text{O}_{7-x}$ have been studied in a transmission electron microscope using 100-, 150-, 200-, 250-, and 300-keV electrons at 83 and 300 K. The disordering of the oxygen atoms and vacancies in the O(4) and O(5) sites in the Cu-O planes during irradiation was monitored by measuring the splitting of the $(1\bar{1}0)$ diffraction spots in the $[001]$ diffraction pattern. The results show that $\text{YBa}_2\text{Cu}_3\text{O}_{7-x}$ is insensitive to 100-keV electron irradiation. Irradiation by higher-energy electrons leads to irradiation-induced oxygen disordering of the oxygen atoms and vacancies, mainly by single displacement events. The excellent fit of the data to a disordering model suggests that the displacement threshold energy for oxygen in $\text{YBa}_2\text{Cu}_3\text{O}_{7-x}$ is around 18 eV and that irradiation-assisted oxygen reordering occurs in $\text{YBa}_2\text{Cu}_3\text{O}_{7-x}$ at 300 K, but not at 83 K.

I. INTRODUCTION

The effects of electron irradiation of $\text{YBa}_2\text{Cu}_3\text{O}_{7-x}$ have been studied with respect to changes in microstructure¹⁻⁴ and properties.⁵ It has been reported that while high-energy electrons (~ 1 MeV) can displace cations, lower-energy electrons can only displace oxygen atoms in the anion sublattice.⁶ Figure 1 is a schematic of the unit cell of $\text{YBa}_2\text{Cu}_3\text{O}_7$. In its orthorhombic state, the lattice parameters a and b take on values of 0.382 and 0.389 nm, respectively. The orthorhombic distortion is due to the ordering of oxygen atoms in the O(4) sites and oxygen vacancies in the O(5) sites (see Fig. 1) in the Cu-O planes. An orthorhombic-to-tetragonal transformation can be brought about either by randomizing the oxygen occupancy between the O(4) and O(5) sites or by loss of oxygen from the sample.¹⁻³ Mitchell *et al.*¹ reported that the former mechanism occurs during low-energy electron irradiation.

The difference in the a and b lattice parameters of $\text{YBa}_2\text{Cu}_3\text{O}_{7-x}$ in the orthorhombic state leads to twinning during transformation on cooling from the high-temperature tetragonal phase. Figure 2 is a schematic of a twin boundary where the a and b lattice parameters are shown to be widely different for illustration purposes. The figure shows that the boundary is along an invariant (110) plane (line AB), common to both lattices, which acts as a mirror plane, inverting the a and b axes across it. This causes the $(1\bar{1}0)$ planes on either side of the boundary (lines CD and EF) to subtend an angle ϕ with each other. The angle ϕ is related to the b/a ratio by the equation³

$$\frac{\phi}{2} = 2 \tan^{-1} \left(\frac{b}{a} \right) - \frac{\pi}{2}. \quad (1)$$

The twinning causes a splitting of the $(1\bar{1}0)$ diffraction spots in a $[001]$ zone axis diffraction pattern [as shown below in Fig. 4(a)], with the split spots subtending an angle ϕ . The magnitude of the angle ϕ , which is related to the b/a ratio by Eq. (1), can thus be used to monitor irradiation-induced oxygen disordering in $\text{YBa}_2\text{Cu}_3\text{O}_{7-x}$ superconductors.

^{a)} Present address: Boston University, Dept. of Manufacturing Engineering, Boston, MA 02215.

II. EXPERIMENT

The irradiation study was carried out on $\text{YBa}_2\text{Cu}_3\text{O}_{7-x}$ filaments supplied by CPS Superconductor Corporation, Milford, MA. The 200- μm -diam filaments were made by a patented polymer dry-spinning process using fine stoichiometric $\text{YBa}_2\text{Cu}_3\text{O}_{7-x}$ powders mixed with a molten polymer. The polymer was burnt out at 500 °C, and the fibers were sintered at 950 °C and annealed for 2 h at 500 °C in oxygen to give superconducting $\text{YBa}_2\text{Cu}_3\text{O}_{7-x}$ filaments with a zero-resistance transition temperature of 90 K.⁷ The filaments were polished from diametrically opposite sides into 30- μm -thick slabs, which were mounted onto slotted copper transmission electron microscopic (TEM) disks and ion milled using 5-keV Ar^+ ions to produce electron transparent thin areas.

Electron irradiations were carried out on $\text{YBa}_2\text{Cu}_3\text{O}_{7-x}$ grains in a Philips CM30 transmission electron microscope using 100-, 150-, 200-, 250-, and 300-keV

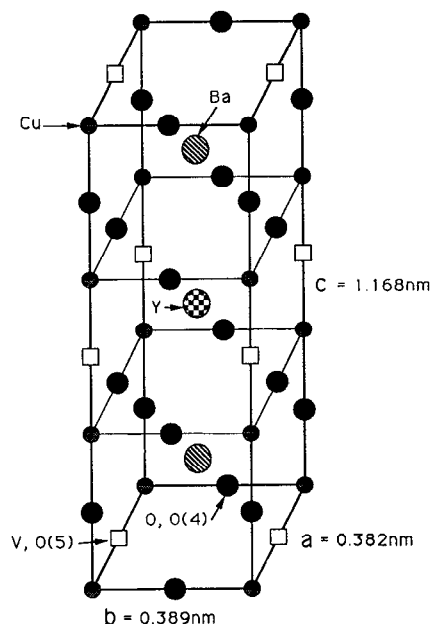


FIG. 1. Schematic of the unit cell of $\text{YBa}_2\text{Cu}_3\text{O}_{7-x}$.

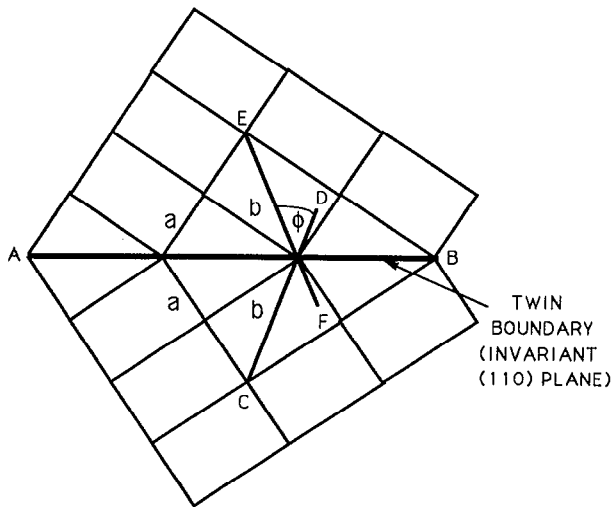


FIG. 2. Schematic of a twin boundary in $\text{YBa}_2\text{Cu}_3\text{O}_{7-x}$, where the difference between the a and b lattice parameters has been exaggerated.

electrons at 83 K. A Gatan double-tilt cooling holder was used with liquid nitrogen to cool the samples. 300-keV electron irradiation was also carried out at room temperature. In each case, the integrated electron-beam current was measured using a Faraday cup built into the sample holder. During the irradiation experiment, the beam was spread to cover just the circular viewing screen of the microscope. The average electron dose rate was calculated, knowing the magnification, screen diameter, and the total beam current. To avoid channeling effects during irradiation, the c axis of the $\text{YBa}_2\text{Cu}_3\text{O}_{7-x}$ grains was tilted at 2° to the electron beam. Care was taken to choose grains that were well connected to the filament to ensure good heat transfer to avoid sample heating. A $50\text{-}\mu\text{m}$ -diam selected-area aperture was used to ensure that the diffraction pattern was obtained from an area smaller than the irradiated area. The $[001]$ diffraction pattern was recorded periodically during irradiation, and the angle ϕ subtended by the split $(1\bar{1}0)$ diffraction spots was measured. The b/a ratio was calculated using Eq. (1). Table I lists the voltages, electron fluxes, temperatures, and total irradiation times used in the experiments.

III. RESULTS

The results of the electron irradiation experiments at 83 K are presented in Fig. 3. The b/a ratio, calculated from the splitting of the $(1\bar{1}0)$ spots, is plotted as a function of irradiation time for different electron acceleration voltages. The figure shows no changes in the b/a ratio during the 100-kV irradiation, indicating that $\text{YBa}_2\text{Cu}_3\text{O}_{7-x}$ is insensitive to 100-keV electrons. Irradiation at higher voltages led to a decrease in the b/a ratio with time, indicating a disordering of oxygen atoms and vacancies at the O(4) and O(5) sites. This was accompanied by microstructural changes in the irradiated $\text{YBa}_2\text{Cu}_3\text{O}_{7-x}$ grains. At the start, all the grains were extensively twinned, with the twin boundaries being quite sharp and well defined. With irradiation, the oxygen disordering led the twin boundaries to become less well defined. Within the time frame of the experiments, the 250- and

TABLE I. Table of irradiation conditions and displacement cross sections.

Voltage (kV)	Flux [$10^{23}e/(\text{m}^2\text{ s})$]	Temperature (K)	Time (min)	σ (barns) (Ref. 11)
100	0.525	83	180	0
150	1.08	83	180	12.94
200	1.94	83	90	20.05
250	2.87	83	75	23.21
300	4.18	83	45	25.00
300	1.25	83	60	25.00
300	4.18	300	60	25.00
300	1.25	300	180	25.00

300-keV electron irradiations led to the complete disappearance of the twin structure, leading to a tetragonal structure ($b/a = 1$), accompanied by a disappearance of spot splitting in the diffraction pattern. Figure 4 shows the changes in the microstructure and $[001]$ diffraction pattern of a grain as a function of 300-keV electron irradiation under a flux of 4.18×10^{23} electrons/ $(\text{m}^2\text{ s})$. Figure 4(a) shows the well-defined, sharp twins of the unirradiated grain, with a large splitting of the $(1\bar{1}0)$ diffraction spots (see arrow). Figure 4(b) shows that after 5 min of irradiation, the twin boundaries are no longer sharp and well defined, and the magnitude of splitting of the $(1\bar{1}0)$ spots has decreased. Figure 4(c) shows that after 45 min of irradiation, both the twins and the splitting of the $(1\bar{1}0)$ spots has completely disappeared, leading to a tetragonal structure.

To study the effect of irradiation flux and temperature on oxygen disordering, grains of $\text{YBa}_2\text{Cu}_3\text{O}_{7-x}$ were irradiated with 300-keV electrons with fluxes of 1.25×10^{23} and 4.18×10^{23} electrons/ $(\text{m}^2\text{ s})$ at both 83 K and room temperature (300 K). Figure 5 shows a plot of b/a ratio versus irradiation time for these experiments. The figure shows that increasing the irradiation dose or decreasing the irradiation temperature leads to a quicker decrease of the b/a ratio with time.

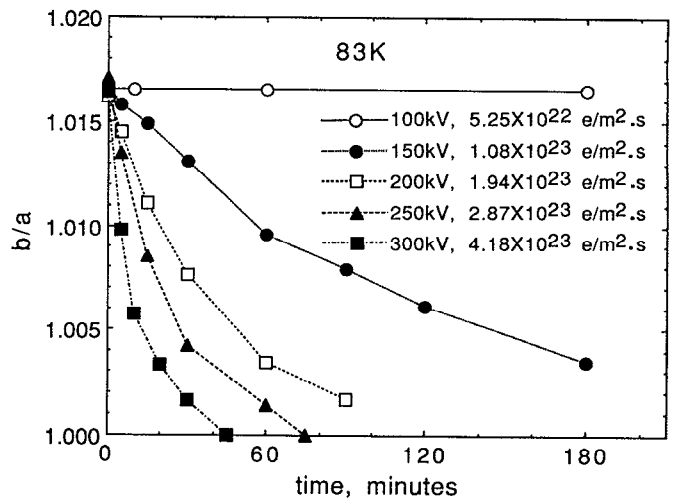


FIG. 3. Plot of b/a ratio vs time for electron irradiation at 83 K.

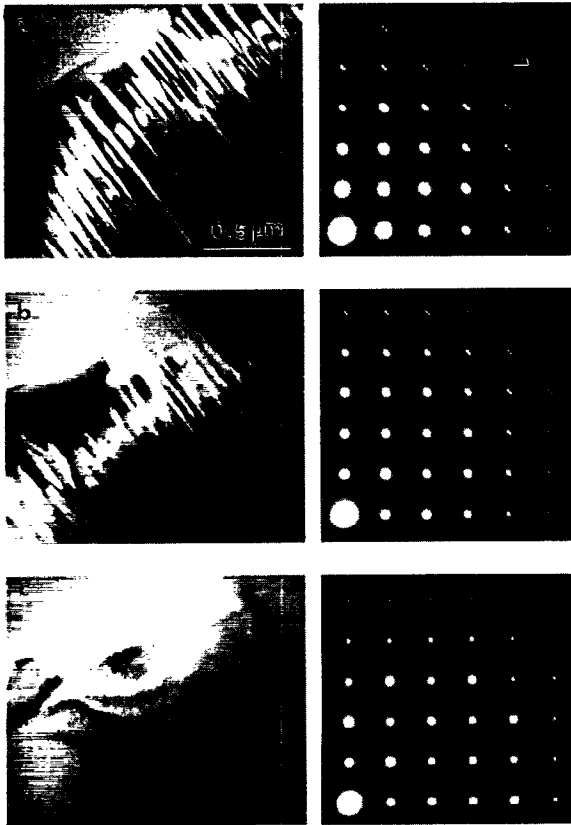


FIG. 4. TEM bright-field micrographs and [001] diffraction patterns of a $\text{YBa}_2\text{Cu}_3\text{O}_{7-x}$ grain after irradiation by 300-keV electrons at 83 K for (a) 0 min, (b) 5 min, and (c) 45 min. The irradiation flux is 4.18×10^{23} electrons/ $(\text{m}^2 \text{s})$. The arrow marks the splitting of the (110) diffraction spots due to twinning in the unirradiated material.

IV. DISCUSSION

The insensitivity of $\text{YBa}_2\text{Cu}_3\text{O}_{7-x}$ to 100-keV electrons has been previously reported in the literature.⁴ This can be understood by considering the maximum energy T_{max} that can be transferred to an atom of mass M by an electron of mass m having an energy E . Taking relativistic effects into account, T_{max} can be calculated as⁸

$$T_{\text{max}} = \frac{2E(E + 2mc^2)}{Mc^2}, \quad (2)$$

where c is the speed of light. The oxygen atoms in $\text{YBa}_2\text{Cu}_3\text{O}_{7-x}$ are the lightest and are most likely to be displaced first by the electrons. The maximum energy transferred to an oxygen atom by 100-keV electrons can be calculated using Eq. (2) to be around 15 eV. The lack of irradiation damage in $\text{YBa}_2\text{Cu}_3\text{O}_{7-x}$ by 100-keV electrons indicates that the displacement threshold energy (T_d) of oxygen atoms is above this value. This is consistent with the observations of Kirk *et al.*,² who found T_d to be around 20 eV, although this value was orientation dependent. Mitchell *et al.*¹ found irradiation damage in $\text{YBa}_2\text{Cu}_3\text{O}_{7-x}$ using 120-keV electrons, indicating that $T_d \leq 18$ eV.

During higher-energy irradiation, the maximum energy transferred to oxygen atoms is larger than T_d , causing oxygen atoms from the O(4) sites to move into vacant O(5)

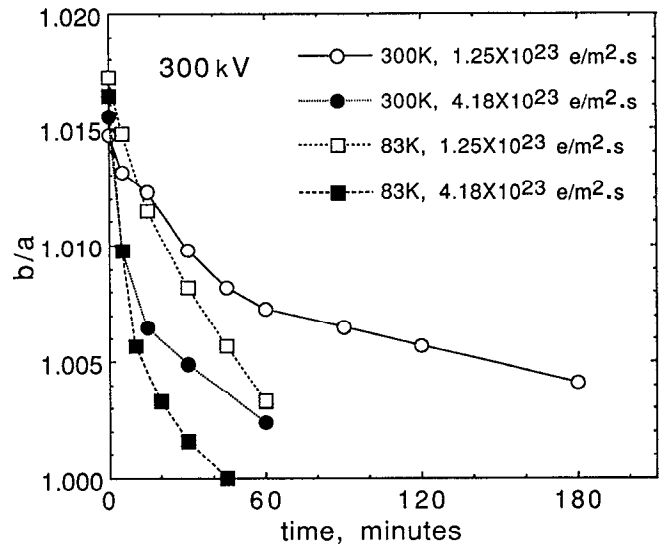


FIG. 5. Plot of b/a vs time for 300-keV electron irradiation at 83 and 300 K (room temperature), at irradiation fluxes of 1.25×10^{23} and 4.18×10^{23} electrons/ $(\text{m}^2 \text{s})$ at both temperatures.

sites (and vice versa). The oxygen atoms and vacancies can be treated as two different species in $\text{YBa}_2\text{Cu}_3\text{O}_{7-x}$ that occupy specific sites [O(4) and O(5), respectively] in the fully ordered (unirradiated) state. The decrease in the ordering of the oxygen atoms and vacancies due to irradiation can be quantified by defining a long-range-order parameter S . In one of the simplest and most useful treatment of order-disorder phenomenon by Bragg and Williams,⁹ the order parameter is defined in terms of the probability of finding a given atom in its correct position. If it is assumed that the b/a ratio of $\text{YBa}_2\text{Cu}_3\text{O}_{7-x}$ varies linearly with the probability of finding an oxygen atom in a O(4) site in a Cu-O plane, S can be defined, based on the Bragg and Williams model, as

$$S = \frac{b/a - 1}{(b/a)_{\text{ord}} - 1}, \quad (3)$$

where $(b/a)_{\text{ord}}$ corresponds to the fully ordered state, when the lattice parameters a and b take on values of 0.382 and 0.389 nm, respectively. It should be noted that in the fully ordered state, S takes on a value of 1, while in the fully disordered (tetragonal) state (random occupancy of oxygen atoms and vacancies, i.e., $b/a = 1$), S becomes 0.

During irradiation, oxygen atoms are knocked out of their correct sites due to ballistic collisions with the energetic electrons. This leads to irradiation-enhanced disordering in $\text{YBa}_2\text{Cu}_3\text{O}_{7-x}$. However, this disordering leads to a large concentration of antisite defects. If these defects are mobile at the irradiation temperature, irradiation-enhanced reordering can take place.¹⁰ Thus, the overall rate of change of the order parameter with irradiation time, $(dS/dt)_{\text{tot}}$, can be written as

$$\left(\frac{dS}{dt}\right)_{\text{tot}} = \left(\frac{dS}{dt}\right)_{\text{dis}} + \left(\frac{dS}{dt}\right)_{\text{ord}}, \quad (4)$$

where the two terms on the right-hand side represent, respectively, the irradiation-induced disordering rate and the

irradiation-enhanced ordering rate.¹⁰ The irradiation-induced disordering rate can be described as

$$\left(\frac{dS}{dt}\right)_{\text{dis}} = -\alpha\sigma JS, \quad (5)$$

where σ is the cross section for oxygen displacement by electrons, J is the electron irradiation flux, S is the instantaneous order parameter, and α is the disordering efficiency which is a measure of replacements per displacement in a collision cascade.¹⁰

The disordering mechanism during irradiation is ballistic, making the process almost independent of temperature. However, since reordering is a thermodynamically driven diffusional process, it is thermally activated and is expected to decrease with temperature. If the irradiation temperature is too low for reordering to occur, the second term on the right-hand side of Eq. (4) is zero. Equations (4) and (5) can then be combined and integrated to give

$$\ln\left(\frac{S}{S_0}\right) = -\alpha\sigma Jt. \quad (6)$$

Thus, in the absence of reordering, a plot of $\ln(S/S_0)$ versus fluence (Jt) for irradiation at each voltage should yield a straight line, whose slope is proportional to the oxygen-displacement cross section for electrons accelerated under the given voltage. Figure 6 is such a plot for 150-, 200-, 250-, and 300-keV electron irradiation at 83 K. The figure shows that the data for electron irradiation at each voltage lie on a straight line, indicating that there is no irradiation-assisted reordering at 83 K. This is due to the lack of mobility of point defects at such low temperatures.

Figure 7 is a plot of $\ln(S/S_0)$ versus displacements per atom (dpa), for oxygen atoms only, which is defined as the product σJt . The values of σ (listed in Table I) were chosen from Oen's compilation¹¹ assuming a T_d value of 18 eV for oxygen atoms. The figure shows that the data for irradiation at all voltages lie on the same straight line. This is consistent with Eq. (6), indicating that the chosen T_d value of 18 eV for

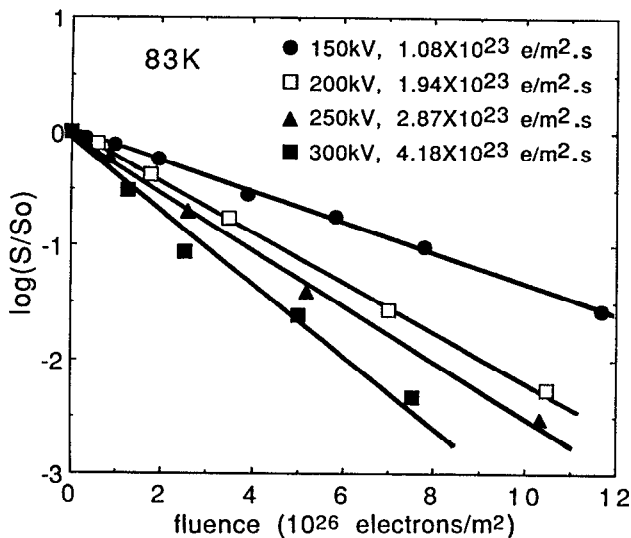


FIG. 6. Plot of $\log(S/S_0)$ vs fluence for electron irradiation at 83 K.

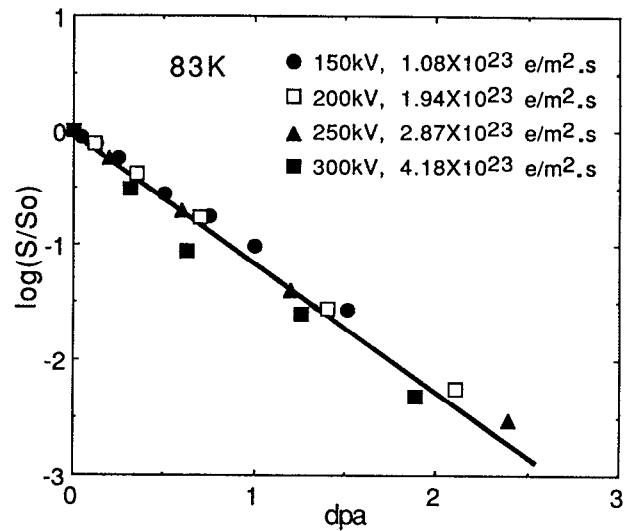


FIG. 7. Plot of $\log(S/S_0)$ vs dpa (oxygen atoms only) for electron irradiation at 83 K.

oxygen is reasonable. The slope of the straight line in Fig. 7 was measured to be 1.14. Equation (6) indicates that the slope is the value of the disordering efficiency α . This is consistent with the reported values of α for electrons in the literature, which are usually around unity.^{8,10} This is an indication that mostly single-collision events are taking place during the irradiation instead of large cascades or replacement collision sequences.

To study the effect of irradiation temperature and electron flux, the data for 300-keV electron irradiation at fluxes of 1.25×10^{23} and 4.18×10^{23} electrons/(m² s) at 83 and 300 K are presented in Fig. 8 as a $\ln(S/S_0)$ versus fluence plot. The figure shows that the data for the 83-K irradiation fall on the same straight line for both fluxes. Thus, at 83 K, the disordering is independent of the dose rate and depends only on the total number of electrons used in the irradiation process. This is further proof that there is no mobility of the point defects at 83 K and consequently no irradiation-assisted reordering. The data for irradiation at 300 K, on the other hand, are flux dependent as seen in Fig. 8. An increase in the irradiation flux causes S to decrease faster with fluence. This is an indication that point defects are mobile in $\text{YBa}_2\text{Cu}_3\text{O}_{7-x}$ at 300 K. For a given fluence, increasing the flux decreases the irradiation time and thus decreases the time for reordering to occur. This is responsible for a quicker decrease in the order parameter with fluence. Thus, under the electron-irradiation conditions used in these experiments, irradiation-assisted reordering does not occur at liquid-nitrogen temperatures, but does so at room temperature. This is an indication of the high mobility of oxygen defects in $\text{YBa}_2\text{Cu}_3\text{O}_{7-x}$, even at room temperature.

The mobility of oxygen defects at room temperature is consistent with recent observations of changes in superconducting behavior of $\text{YBa}_2\text{Cu}_3\text{O}_{7-x}$ with aging at room temperature, both for irradiated material and oxygen-deficient material. Marwick *et al.*¹² found that the increment in room-temperature resistivity of $\text{YBa}_2\text{Cu}_3\text{O}_{7-x}$ caused by ion bombardment can be recovered completely by annealing at

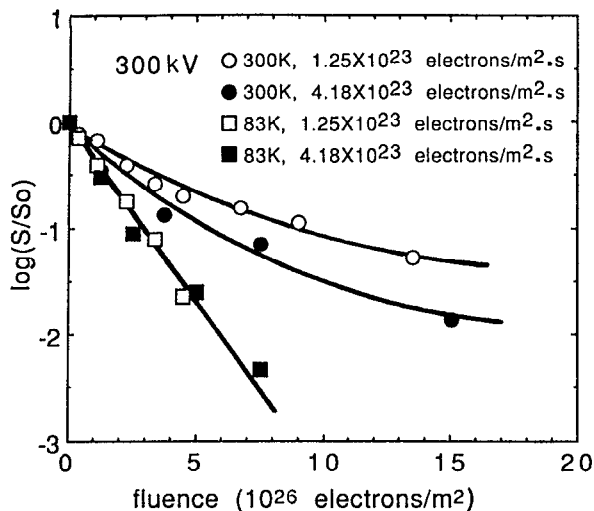


FIG. 8. Plot of $\log(S/S_0)$ vs fluence for 300-keV electron irradiation at 83 and 300 K, at irradiation fluxes of 1.25×10^{23} and 4.18×10^{23} electrons/(m^2 s) at both temperatures.

room temperature, if the damage dose is small. Veal *et al.*¹³ and Jorgenson *et al.*¹⁴ found that, in oxygen-deficient $YBa_2Cu_3O_{7-x}$ prepared by quenching from 500 °C into liquid nitrogen, the superconducting transition temperature could be increased by annealing at room temperature. This was ascribed to local ordering of oxygen atoms around the Cu sites. Such reordering at ambient temperature has also been observed *in situ* for materials disordered by electron irradiation.¹ All these observations support the contention that oxygen is mobile in $YBa_2Cu_3O_{7-x}$ at ambient temperatures.

V. CONCLUSIONS

Electron-irradiation experiments were carried out in a transmission electron microscope on thin foils of bulk $YBa_2Cu_3O_{7-x}$ using 100-, 150-, 200-, 250-, and 300-keV electrons at 83 K and 300-keV electrons at 300 K. The experiments showed that $YBa_2Cu_3O_{7-x}$ is insensitive to 100-keV electrons. This is because the maximum energy transferred by the 100-keV electrons to an oxygen atom is below its threshold displacement energy. Irradiation with the higher-energy electrons led to a disordering of the oxygen atoms and vacancies in the O(4) and O(5) sites in the Cu-O planes, leading to a change in the b/a ratio. This change was

monitored by measuring the splitting of the (1 $\bar{1}$ 0) diffraction spots in a [001] diffraction pattern. A long-range-order parameter was defined to characterize the ordering of the oxygen atoms and vacancies in the Cu-O planes. An excellent fit of the data to an order-disorder model indicates that point defects are not mobile in $YBa_2Cu_3O_{7-x}$ at 83 K as seen by the lack of irradiation-assisted reordering at that temperature. The data also indicates that the threshold displacement energy of oxygen atoms in $YBa_2Cu_3O_{7-x}$ is around 18 eV and the disordering is mainly due to single-collision events. The lack of irradiation-assisted disordering at 83 K was further confirmed by the insensitivity of the change in order parameter with fluence to the irradiation flux during 300-keV electron irradiation. However, at 300 K, the change of order parameter with fluence was dependent on the flux, indicating that oxygen defects are mobile in $YBa_2Cu_3O_{7-x}$ at 300 K, leading to irradiation-assisted reordering at room temperature.

ACKNOWLEDGMENTS

The authors would like to thank Dr. J. W. Halloran of CPS Superconductor Corporation for providing the superconducting $YBa_2Cu_3O_{7-x}$ filaments used in this study. This work has been supported in part by the U.S. Department of Energy, Office of Basic Energy Sciences, and the Los Alamos Superconductivity Pilot Center.

¹ T. E. Mitchell, T. Roy, R. B. Schwarz, J. F. Smith, and D. Wohlleben, *J. Electron Microsc. Tech.* **8**, 317 (1988).

² M. A. Kirk, M. C. Baker, J. Z. Liu, D. J. Lam, and H. W. Weber, *Mater. Res. Soc. Symp. Proc.* **99**, 209 (1988).

³ G. Van Tendeloo and S. Amelinckx, *J. Electron Microsc. Tech.* **8**, 285 (1988).

⁴ F. W. Clinard, E. M. Foltyn, R. J. Livak, D. E. Peterson, W. A. Coghlan, and L. W. Hobbs, *J. Appl. Phys.* **65**, 12 (1989).

⁵ N. Moser, A. Hofmann, P. Schüle, R. Henes, and H. Kronmüller, *Z. Phys. B* **71**, 37 (1988).

⁶ D. M. Parkin and M. Nastasi, *Mater. Res. Soc. Symp. Proc.* **128**, 351 (1989).

⁷ J. W. Halloran (private communication).

⁸ K. C. Russell, *Prog. Mater. Sci.* **28**, 229 (1984).

⁹ W. L. Bragg and E. J. Williams, *Proc. R. Soc. London A* **145**, 699 (1934).

¹⁰ K. Y. Liou and P. Wilkes, *J. Nucl. Mater.* **87**, 317 (1979).

¹¹ O. S. Oen, "Cross Section for Atomic Displacements in Solids by Fast Electrons," Report No. ONRL-4879 (1973).

¹² A. D. Marwick, G. J. Clark, K. N. Tu, D. S. Lee, C. Lee, U. N. Singh, J. Doyle, and J. J. Cuomo, *Nucl. Instrum. Methods B* **40/41**, 612 (1989).

¹³ B. W. Veal, H. You, A. P. Paulikas, H. Shi, Y. Fang, and J. W. Downey, *Phys. Rev. B* **42**, 4770 (1990).

¹⁴ J. D. Jorgenson, S. Pei, P. Lightfoot, H. Shi, A. P. Paulikas, and B. W. Veal, *Physica C* **167**, 571 (1990).